STUDY ON THE MECHANISM OF INDOOR TEMPERATURE AND HUMIDITY CHANGE IN THE SUNKEN SOLAR GREENHOUSE DURING THE SMOTHERING PERIOD

/

下沉式日光温室闷棚期间温湿度变化机制的研究

Weiwei CHENG [1)], Xin YOU [2)], Tao TIAN [2)], Jiaxuan LU[2)], Junlin HE [2)], Zhouhua LIU [*1)], Fei HAN [1)]
[1)] Shanxi Agricultural University, College of Urban and Rural Construction, Taigu / China
[2)] Shanxi Agricultural University, College of Agricultural Engineering, Taigu / China
Tel: +86-0354-6287420; E-mail: lzh6175305@163.com
Corresponding author: Zhonghua LIU
DOI: https://doi.org/10.35633/inmateh-69-20

***Keywords:** sunken solar greenhouse, solar radiation, temperature and humidity, sterilization*

ABSTRACT

A sunken solar greenhouse is the original type of greenhouse in China, its soil wall thermal storage performance is better and low cost. Higher benefits of stereoscopic planting in sunken solar greenhouses, while repeated use of the substrate can produce pathogens, so high-temperature smothering is used for sterilization in the summer months of June to August. To investigate the mechanism of indoor temperature and humidity variation and fungicidal effect in a sunken solar greenhouse, a single cross-sectional test of temperature and humidity in sunken solar greenhouse during the smothering period was conducted using wireless sensors. The results showed that: The maximum value of indoor temperature at noon was 69.5°C the temperature value of all measurement points was greater than 50°C for 3h, when removing the measurement points at the upper surface of the ground, the relative humidity value of other measurement points was less than 60% for 5h. During the daytime period, when the indoor temperature is greater than 28°C in the interval 7:00-12:00, the initial relative humidity value of each measurement point is located at 70%-85%; when the weighted temperature of each measurement point starts to rise at a rate of 1.1°C/10min, the weighted humidity of each measurement point declining is 1.3%/10min; the determination of the rate of change of indoor temperature and humidity during the daytime and the starting value can provide a basis for indoor plants to take measures to sterilize at high temperature.

摘要

下沉式日光温室是我国原创型式的温室，其土质墙体储热性能好且造价低廉。在下沉式日光温室中采用立体栽培收益较高，而基质重复使用会产生病菌，因此在夏季 6-8 月份采用高温闷棚杀菌。为探究下沉式日光温室室内温湿度变化机制和杀菌效果，利用无线传感器对闷棚期下沉式日光温室的温湿度进行单横截面试验，结果显示：室内温度在中午时刻的最高值为 69.5℃，所有测点的温度值大于 50℃的时长为 3h，去除地面上表面处测点时，其他测点的相对湿度值小于 60%的时长为 5h；白天期间，在 7:00-12:00 时间段内，当室内温度都大于 28℃，各测点的初始相对湿度值位于 70%～85%，当各测点加权温度以 1.1℃/10min 速度开始上升，各测点加权湿度的下降速率为 1.3%/10min，白天期间室内温湿度变化速率和起始值的确定，可为室内有植物采取闷棚的措施提供依据。

INTRODUCTION

The solar greenhouse is an essential agricultural facility in China, which is often referred to as "conservation farming," "controlled environment farming," "greenhouse farming," and "facility farming". (*Steven et al, 2017; Jia et al, 2016*). There are three types of facility farming facilities in China, namely plastic greenhouses, solar greenhouses, and attached greenhouses, among which solar greenhouses are the original agricultural facilities in China (*Peng P et al., 2019*). Moreover, the COVID-19 pandemic is threatening the world's food security, depriving 265 million individuals of food by the end of 2020 (*Lal R., 2020*).

Greenhouses are used to mitigate the harsh weather conditions and allow for a full year-round production of crops (*Morshed W. et al., 2022*) by controlling the microclimate and ensuring that the crops acquire the required level of temperature, humidity, water, and light (*Ghani S. et al., 2019*).

[1] *Weiwei Cheng, As Lec.Ph.D. Eng; Xin You, M.S. Eng; Tao Tian, M.S. Eng; Jiaxuan Lu, M.S. Eng; Junlin He, Prof.Ph.D.Eng; Zhonghua Liu Asoc.Prof.Ph.D. Eng; Fei Han, M.S. Eng;*

A solar greenhouse is a facility that uses solar energy resources so that the indoor air absorbs solar heat during the daytime and the indoor walls and soil absorb heat during the day and exotherm at night, thus providing a suitable microclimate inside the greenhouse. The sunken solar greenhouse is an original structural type of greenhouse in China, and its outstanding advantages are low cost and good heat storage performance, which is very suitable for Chinese vast land and weak economy (*Zhang LH et al., 2010*). The temperature value inside the sunken solar greenhouse is 2°C higher than that of the greenhouse built on flat ground, and the sunken solar greenhouse can also reduce the influence of external low temperature on the soil, and the low-temperature value of its south margin area is greater than that of the south margin area of the non-digging solar greenhouse, so the application of the sunken solar greenhouse is widely promoted in production. The sunken solar greenhouse originated in northeastern China to improve the thermal insulation performance of the greenhouse, and the initial concave depth of the sunken solar greenhouse was 0.5-1 m. At the present stage, the concave depth is 1.2-2 m, equivalent to a 1-m-high wall around the southern ground margin, which is better than the general greenhouse thermal insulation effect.

Substrate stereo culture and soil cultivation can be used in daylight greenhouses, which can cause the soil and substrate to carry pathogens during repeated planting. Continuous planting of strawberries in the soil or substrate provides conditions for the development of a large number of pathogens (*Chen P et al., 2020*), which can lead to a reduction in yield and, at a later stage, to the death of the strawberry plant. Smothering means that during the summer period, no plants are grown indoors and all air vents in the solarium are closed to take advantage of the high indoor temperatures generated by the solar radiation absorbed by the greenhouse to kill harmful bacteria. To alleviate the trend of soil deterioration and improve the growing environment of crops, high-temperature smothering is usually carried out during the high-temperature crop vacancy period from June to August in summer, i.e., the greenhouse is sterilized by using high temperature above 70°C (*Shi L.J. et al., 2021*). *Li J.C. et al*., *(2015),* studied the physicochemical characteristics of soil during the high-temperature smothering period and found that irrigation smothering can help promote soil restoration, which can increase yield and improve economic efficiency, and can be actively applied in continuous crop production. After smothering there is also a reduction in beneficial bacteria such as Phytophthora and Helicobacter nitrificans, which play an important role in the nitrogen cycle in the soil (*Sun B.et al., 2020*). Smothering can be effective in controlling root knot nematodes and affecting the microbial community structure in the soil (*He Wei et al., 2022*). The result (*Hu Q.Q. et al., 2015*) showed that the plants in the irrigation and high-temperature smothering treatment were better than the control in terms of plant height, stem thickness, leaf growth and fruit quality. It was confirmed that adding corn straw combined with high-temperature smothering, not only has a strong disinfection effect on the soil, but also accelerates the decomposition of straw, increases soil organic matter content, reduces soil salt content, and improves the soil microbiological environment (*He Z.G. et al., 2018*). *Fu G.H.* and *Liu W.K., (2016*), verified that the temperature of the substrate rooting area in the heliostat was significantly and positively correlated with the daily indoor and outdoor temperatures. Therefore, the studying of indoor temperature and humidity during the smothering period of sunken solar greenhouse can provide theoretical data and reference for farmers to smother their greenhouses for sterilization. The process of sunken solar greenhouse smothering in the three-dimensional planting method is as follows: the three-dimensional planting facilities are covered with plastic film, the substrate is filled with water, all indoor wind vents are closed, and the quilt is not pressed into the shed.

MATERIALS AND METHODS

Greenhouse tested

The sunken solar greenhouse was smothered from June 30, 2019 to August 7, 2019. The tested greenhouse was a sunken three-dimensional planting solar greenhouse, as shown in Figures 1 and 2. The greenhouse was north-facing, with a length of 108 m and a span of 12 m. The sunken solar greenhouse had a concave depth of 1.2 m on the south wall, a width of 1.1 m on the south aisle, and a width of 1.2 m on the north aisle. The external height of the rear wall of the sunken solar greenhouse is 4.3 m, and the ridge height is 5 m. The width of the north wall is 6 m at the bottom and 2 m at the top. The main bearing skeleton is made of elliptical steel pipe with a skeleton spacing of 1 m, and the covering material is plastic film.

All air vents of the greenhouse were closed during the smothering period, the base tank was filled with water, the water outlet at the bottom of the base tank was closed, the A-frame was covered with plastic film, and the greenhouse was shown in Figure 1.

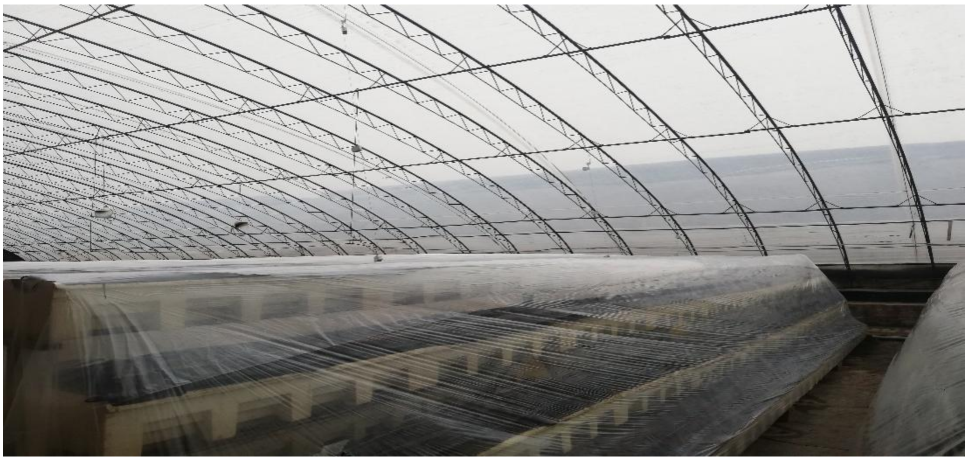

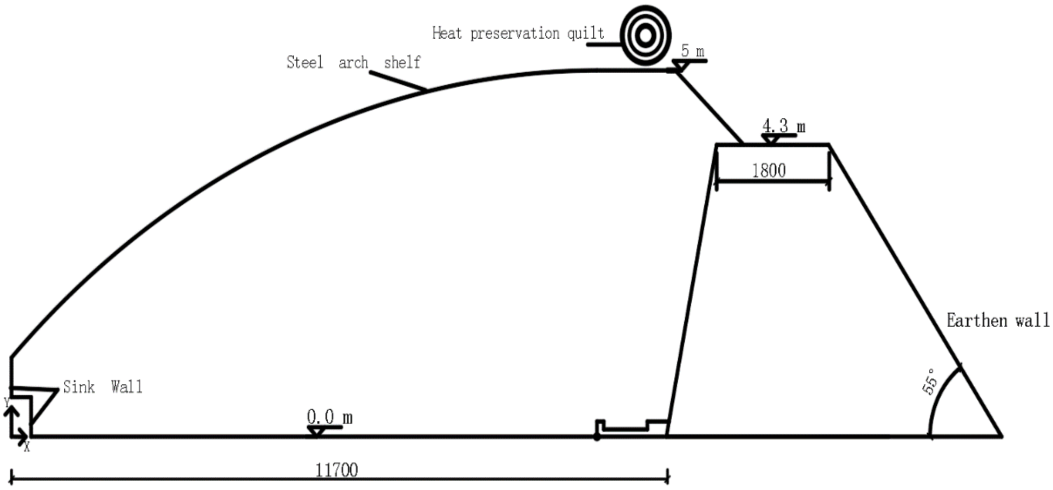

Fig. 1 - Sunken Solar Greenhouse and cross-sectional view

Theoretical basis

Area heat received by space points in indoor air (q_{total})(*Cheng W.W. et al., 2021*):

$$q_{total} = \alpha \cdot S_{total} = S_1' \cdot T_1 \cdot \alpha \cdot (1 - \eta \cdot H_{aze}) + S_2' \cdot T_1 \cdot \alpha \cdot (1 - \eta) \tag{1}$$

where:

q_{total} is the total solar radiation at a point in the indoor space, W/m^2;

S_1' - the direct solar radiation illumination of the light passing through the atmosphere to the outer surface of the greenhouse membrane, W/m^2;

S_2' - the solar scattering radiation illumination of the light passing through the atmosphere to the outer surface of the greenhouse membrane, W/m^2;

T_1 - the direct light transmittance of the film at different roof angles, %;

T_2 - the transmittance of scattered light of the film at different roof angles, %;

S_{Qs} - the amount of scattered solar radiation received by space point Q in the greenhouse W/m^2.

S_{Qz} - the amount of direct solar radiation received by space point Q in the greenhouse, and the incidence angle of light is θ, W/m^2.

H_{aze} - the Haze of covering material, %; q is heat per unit area, W/m^2;

S_{total}- the total solar irradiance of the outdoor horizontal plane, W/m^2;

A_s - the greenhouse ground area, m^2;

α - the correction coefficient of the heated area;

ρ - the indoor sunshine reflectance;

η - the influence coefficient of point scattering quantity, which is related to the coordinate values of y and z of the section where it is located, and has nothing to do with the longitudinal coordinate *x*.

Testing instruments

Wireless sensors are used to collect data at different heights. The indoor temperature and humidity collection instrument in the solar greenhouse is an HT59-Li-A1 wireless temperature and humidity collector developed by Shenyang Weien Technology Co., LTD and calibrated by Liaoning Provincial Institute of Metrology Science, and coordinated with WG59 gateway. The wireless temperature and humidity collector transmits the temperature and humidity data collected by the wireless temperature and humidity collector to the WG59 gateway through GPRS. The WG59 gateway collects the private network data to the cloud server through the Internet and obtains the data information through mobile phones or computers. Temperature measurement range of wireless temperature and humidity collection instrument: 40 ~ 85^{o}C, accuracy: ±0.2° (0 ~ 65^{o}C), ±1° (other temperature range). The transmission period of the wireless temperature and humidity collector and the gateway is 6 minutes, and the data is measured and transmitted continuously 24 hours a day.

Testing methods

To explore the variation law of temperature and humidity in the greenhouse, the duration of indoor high temperature and the maximum indoor temperature value during the stuffy greenhouse period, the temperature and humidity of the sunken solar greenhouse during the stuffy conservatory were measured experimentally. Because the high temperature and high humidity will damage the sensor, the single cross section method is used to measure the temperature and humidity value of sunken solar greenhouse. The cross-section 30 m from the west wall was selected as the cross-section to be measured, and the coordinate system was established in the cross section. The intersection point between the indoor ground and the extension line of the sinking wall was 0, the vertical upward was the positive *y* axis, and the north direction of the line of intersection between the interior floor and the cross section is the *x* axis. The coordinate system was established, as shown in Figure 2. Four positions were selected along the section to be measured from south to north, and s-type hooks were hung on the lower chord of the steel truss at the corresponding positions. The height of the s-type arches was 300 mm, and wire ropes were suspended at the lower end of the arches. Wireless temperature and humidity acquisition instruments were arranged at different heights of the wire ropes. The measurement lines are numbered 1, 2, 3, and 4, and the number of sensors placed on the corresponding lines is 4, 5, 5, and 5. The vertical and horizontal spacing is shown in Table 1. A wireless temperature recorder is placed 1.5 m outside to measure outdoor temperature and humidity.

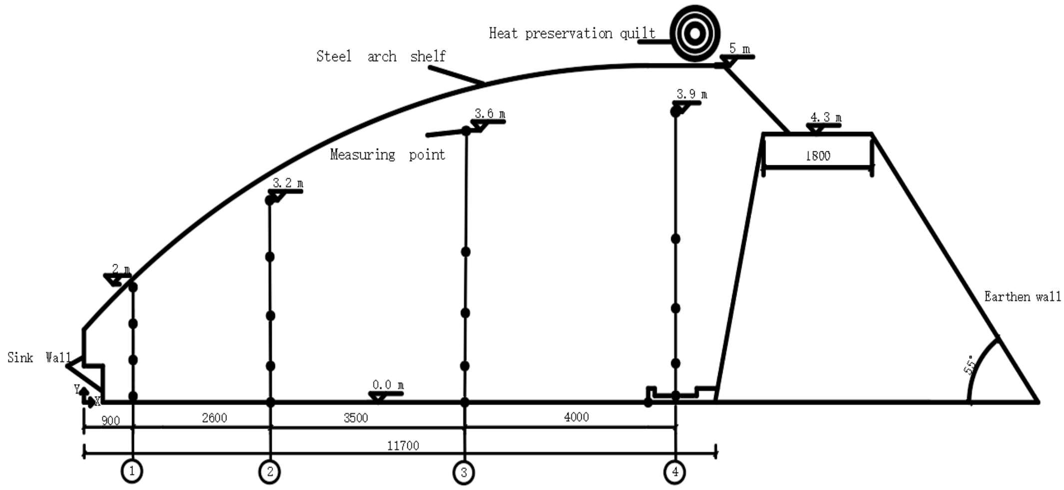

Fig. 2 - Schematic diagram of survey line layout indoor

Table 1

Height from the measuring point to the indoor ground during the closed canopy period (m)

Line number	1	2	3	4
The x coordinate [m] / **Measurement point number**	0.9	3. 5	7	11
1	2.0	3.2	3.6	3.9
2	1.6	2.4	2.4	2.4
3	0.8	1.6	1.6	1.6
4	0	0.8	0.8	0.8
5		0	0	0

Data processing methods

Origin 8.5 and Excel 2010 were used for data analysis and 2D chart making.

RESULTS AND DISCUSSION

According to the theoretical formula (1): the smaller the horizontal distance from the north wall, the higher the height from the indoor ground, the higher the temperature would be. The temperature value of the measuring point closest to the wall on the north side and the maximum indoor ground height were selected for analysis, that was, the temperature value of measuring point 4-1. In the middle of July 2019, the highest temperature value of the 4-1 measuring point was 69.5°C, 14:30 on July 13, 2019. At this time, it was sunny outdoor, and the outdoor temperature had the lowest value of 19°C and the highest value of 38°C.

The change law of indoor temperature

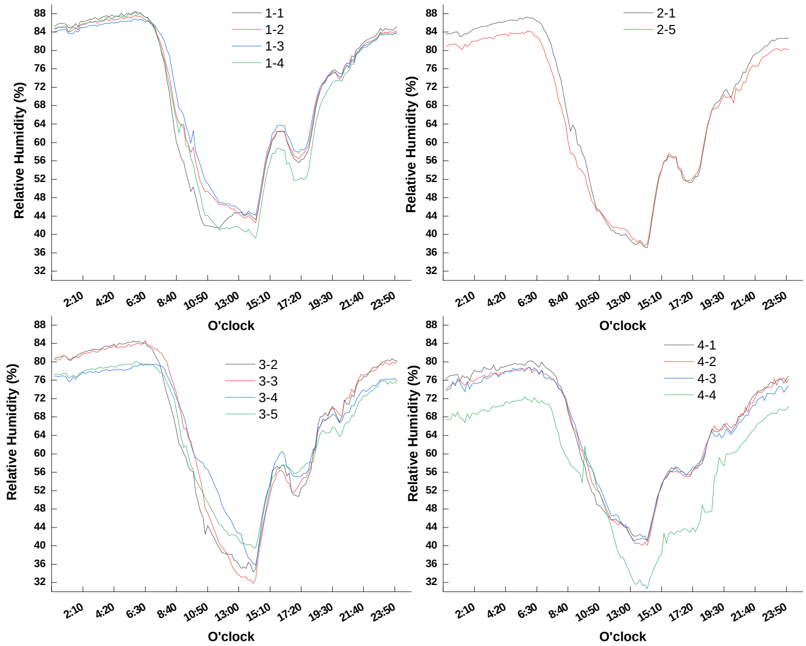

Fig. 3 - The curve of temperature outdoor and measuring points indoor with time

Figure 3 showed that the temperature difference between indoor and outdoor was significant. The maximum temperature difference between indoor and outdoor occurred at 14:10, and the maximum temperature difference between indoor and outdoor was 31.1 °C. At night (00:00-6:00), the temperature value of each measuring point decreased linearly with time. The smaller the indoor ground surface height was, the higher the temperature value was. During this period, indoor air exchanged heat with outdoor through plastic shed film, and indoor wall and indoor soil continued to release heat. Not considering the temperature of the indoor floor, the nighttime temperature difference between measuring points on Line 3 was between 0.1 °C and 0.5 °C. The nighttime temperature difference between measuring points on measuring line 4 was between 0.1 °C and 0.5 °C. At the same time and on the same measuring line, the temperature difference at night between the measuring point at 0 m on each measuring line and the adjacent measuring point was 0.8 ~ 1.2 °C on measuring line 1, No. 3 measuring line was 0.8 ~ 1.1 °C and measuring line 4 was 0.8 ~ 1.1 °C. Therefore, at the same time, the temperature difference at night between the measuring point 0 m away from the upper surface of the indoor ground and the measuring point 0.8 m away from the upper surface of the indoor ground on the same measuring line was more significant than that between the measuring points above 0.8 m.

Between 6:00 and 14:30, the temperature curve of indoor measuring points increased and reached the maximum at about 14:30. The indoor temperature increased because of solar radiation, and the wall and soil on the north side of the room were in an endothermic state. During this period, the temperature of each measuring point increased by 36-43 °C. The maximum temperature of each measuring point on the same measuring line was the point in the middle of the measuring line and the temperature value of the measuring point at 0m on the ground surface was the smallest. This is due to the large difference between indoor and outdoor temperature, resulting in more significant indoor heat loss.

The maximum temperature difference between other measuring points on the same measuring line was 1.2 °C on line 1, 2.9 °C on line 3 and 2.2 °C on line 4, except for the measuring point at 0 m above the ground surface (0 m away from the indoor ground). 14:10 The temperature difference between the temperature value of the measuring point at 0 m on the same measuring line and the adjacent measuring point (the height between each measuring line and the upper surface of the indoor ground is 0.8 m) was 5.6 °C on Line 1, 5.1 °C on Line 3 and 6.6 °C on Line 4. Therefore, it could be seen that the temperature difference between measuring points at 0 m above the indoor ground surface and adjacent measuring points (0.8 m above the indoor ground surface) was more significant than that between measuring points above 0.8 m above the same measuring line.

From 14:00 to 14:30, the temperature of most of the measuring points reached the maximum value, and the time difference of the temperature of each point reaching the maximum value was less than 20 min. The maximum temperature of the indoor measurement point was 69.5 °C, and the outdoor temperature value at the same time was 38.4 °C. At this time, it was the ultimate outdoor temperature, and the difference between indoor and outdoor temperature was 31.1 °C, indicating a significant indoor and outdoor temperature difference. From 14:00 to 14:30, the lowest temperature of each measuring point was 57.1 °C, which was a 4-5 measuring point, located on the upper surface of the indoor ground in the north corridor. The period when the temperature value of all measuring points was greater than 40 °C was 9:50-19:00, up to 9h; The period when the temperature value of all measuring points was greater than 50 °C was 11:40-15:00 for 3 hours. The duration of maintaining room temperature above 40 °C was similar to that of Li JC's research (*Li J.C., 2015*), and its research results showed that it could meet the sterilization requirements.

From 14:30 to 16:00, the temperature values of each measuring point gradually decreased, because the outdoor light intensity gradually reduced, and the heat loss of the greenhouse was more significant than the heat absorption, so the indoor air temperature decreased. From 16:00 to 18:00, the temperature value of each measuring point increased slightly, due to the increase of outdoor light intensity, and the indoor heat absorbed was more significant than the heat loss due to the temperature difference between indoor and outdoor. The temperature values of each measuring point decreased linearly with time from 19:00 to 24:00. To verify whether it was a linear model, a scatter plot was made for the temperature values of each measuring point from 19:00 to 24:00 , and a linear fitting was conducted. The fitting coefficient R^2 was ≥0.9, indicating an excellent proper relationship.

Table 2

The maximum temperature changes at different heights in the room (m)

Height of the point [m]	**Line number**	1	2	3	4
	The *x* coordinate [m]	0.9	3.5	7	11
0		56.6	-	64	57.1
0.8		62.2	-	69.5	63.4
1.6		63.4	-	67.9	64.1
2.0		62.8			
2.4		-	66.1	-	63.9

It can be seen from Table 2 that the temperature value of the measuring point 0 m away from the upper surface of the indoor ground was the lowest among all measuring lines, and the temperature difference with the adjacent measuring point was the largest. At the same time and line, the temperature of the most significant point was not the biggest point with indoor ground height on the line 3, it was because of the A-frame, which covered strawberries with plastic wrap during the smothering period. No. 3 line measuring point was located on the outer surface of the plastic films, plastic films having a reflection effect on indoor sunlight, in the middle point to receive plastic greenhouse films of reflected light. Therefore, the temperature value of the measuring point at the medium height of No. 3 measuring line was higher. At the same height, with the increase of Y-axis coordinates, the temperature first increased and then decreased. The temperature at line 3 was the highest. This was because line 3 was located in the middle of the greenhouse and received more reflected light from plastic shed film, resulting in a higher temperature at the measuring point of this line.

The change law of indoor relative humidity

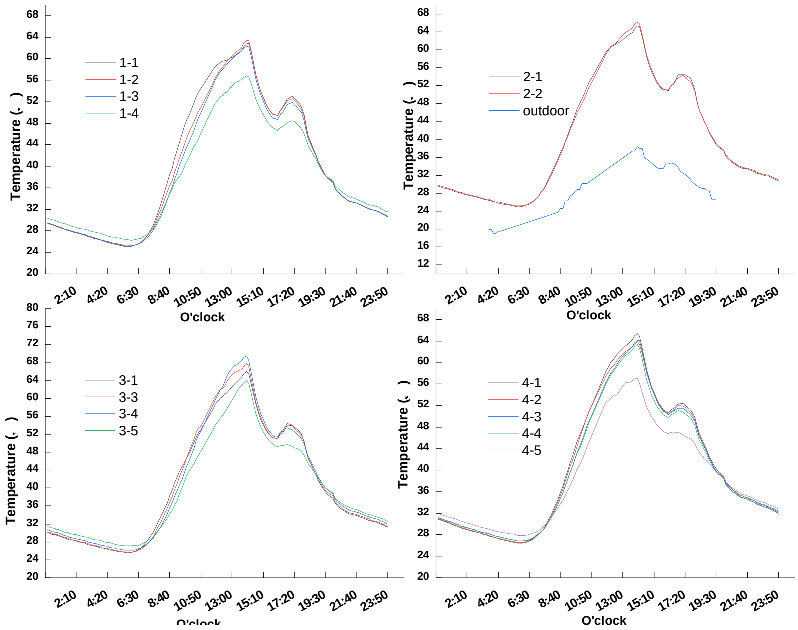

Fig. 4 - Curve of relative humidity measuring points with the time

Figure 2 and Figure 4 showed that: (1) the relative humidity of indoor air was relatively high from 00:00 to 6:00, and the relative humidity of each measuring point was above 67%, and the highest was 90%. During this period, with the decrease of indoor temperature, the relative humidity of each measuring point gradually increased, and the relative humidity of each measuring point decreased between 1.6% and 4.7%.

(2) Between 6:00 and 12:00, the indoor humidity curve decreased, and the lowest relative humidity value was between 30% and 45%; the inflection point of relative humidity at each measuring point was different. The inflection point of most measuring point curves was 6:20, and the latest measuring point of an inflection point in the measuring point curve was the measuring point at 0 m on the surface of the ground, and its time was 8:00. At the inflection point of the relative humidity value of each measuring point over time, the temperature value of each indoor measuring point was more significant than 25°C. During 6:20-7:20, the average temperature drop rate of each measuring point was 0.27°C/10min, and the average relative humidity drop rate of each measuring point was 0.43%/10min. The time when the relative humidity of each measuring point began to drop significantly was 7:30, and the temperature of each indoor measuring point was higher than 29°C. Between 6:00 and 12:00, the average decrease rate of relative humidity of all measuring points was 1.3%/10min, and the average rise rate of the temperature of each measuring point was 1.1 °C/10min.

(3) From 12:00 to 14:00, the relative humidity at each measuring point decreased at a slowly rate. During this stage, the average temperature rise rate at each measuring point was 0.5°C/10min, and the average decrease rate of relative humidity was 0.37%/10min. At this time, the temperature value of all measuring points is more significant than 57°C, and the relative humidity value of all measuring points (excluding 1-4 measuring points and measuring points near the ground) was between 40% and 46%. This was because measuring points 1-4 are located at the beginning of planting, below the upper water pipe and return water pipe of drip irrigation, and there was leakage at the interface. Therefore, the relative humidity value of the measuring points here was around 59%. When 1-4 measuring points were removed, the relative humidity of other measuring points was less than 60% for 5 h, and the relative humidity of other measuring points was less than 50% for 2.2 h.

(4) From 14:00 to 16:00, the relative humidity value of each measurement point increased, which was because outdoor light intensity decreased, indoor air heat absorption was less than the energy loss of indoor and outdoor temperature, resulting in indoor temperature decrease and relative humidity increase. From 16:00 to 17:30, the outdoor light intensity increased, leading to indoor temperature increase, and indoor relative humidity value decreased during this period.

(5) The relative humidity of each measuring point increased from 18:00 to 24:00, and the increased range of relative humidity during this period was more significant than that during 00:00 to 6:00. From 18:00

to 24:00, the average relative humidity drop value of all measuring points was 19.8%, and the average temperature drop value of all measuring points during this period was 12.9°C.

It can be seen that during the stuffy greenhouse period, the indoor relative humidity curve with time and the indoor temperature curve with time in the sunken solar greenhouse showed opposite laws in the same period, and the humidity was at the lowest value, when the temperature was the highest. The relationship between indoor temperature and humidity should be established during the stuffy shed period, to provide a theory for production practice.

The relation between indoor temperature and relative humidity

As can be seen from the change law of indoor relative humidity, when the indoor air temperature was higher than 29°C, the relative humidity of indoor air decreased significantly with the increase of indoor air temperature. Therefore, the relative humidity and temperature at different measuring points from 7:30 to 12:00 were established, providing a theoretical reference for the measures of greenhouse temperature rise and humidity reduction. Since water droplets on the inner surface of the greenhouse film would drop to the ground, resulting in high humidity on the surface of the greenhouse, the relationship between relative humidity and temperature at the measuring point 0 m on the surface of the indoor ground was not considered.

The relative humidity value of each measurement point during 7:20-12:00, on July 13, 2019 was taken as the *Y*-axis, and the temperature value of the corresponding measurement point was taken as the *X* value. The temperature and humidity scatter plot was drawn and linear fitting was carried out. The temperature and humidity curve equation of each measurement point during 7:20-12:00 is shown in Table 3.

Table 3

Temperature and humidity relation diagram of different measuring points from 7:30 to 12:00

Code number	Fitting equation	The correlation coefficient
1-1	y=-1.3405x+115.45	0.94
1-2	y=-1.2788x+115.4	0.96
1-3	y=-1.3502x+119.5	0.97
2-1	y=-1.3193x+116.51	0.97
2-2	y=-1.3285x+116.61	0.98
3-1	y=-1.1763x+107.81	0.97
3-3	y=-1.2778x+113.76	0.98
3-4	y=-1.4094x+122.96	1
4-1	y=-1.2027x+112.14	0.98
4-2	y=-1.1924x+111.58	0.98
4-3	y=-1.1789x+110.6	0.99
4-4	y=-1.1282x+109.29	1

N-M in Table 3 represents the *M* measuring point on measuring line *N*, for example, *4-3* represents the 3rd measuring point on measuring line 4.

It can be seen from Table 3 that: during the period from 7:30 to 12:00, the curve fitting of relative humidity and temperature at different measuring points was good, and the correlation coefficient R^2 was > 0.94. In this period, over time, the indoor light intensity increased, and the relative humidity of the indoor measurement point and the temperature of the corresponding measurement point were linearly negative correlation, that was, with the increase of temperature, the indoor relative humidity gradually decreased. At different measuring points, the change rate of the curve equation was between -1.1 and -1.4. The temperature of each measuring point reached 57°C at noon, and the humidity of each measuring point at this time was less than 50%.

In order to study the relationship between temperature and humidity in the sunken solar greenhouse during the period from 7:30 to 12:00, the weighted average value of the change rate of temperature and humidity curves at each measuring point was calculated, and the formula was as follows:

$$\bar{v} = \frac{\sum y_i z_i v_i}{y_i z_i} \tag{2}$$

In formula (2), y_i and z_i were the coordinate values of the measuring points, and were the change rates of the relative humidity and temperature curves of the measuring points. Thus, the weighted average speed can be obtained as -1.23. During the stuffy period, the indoor temperature increased by 1°C, and the indoor relative humidity decreased by 1.23%. At 7:00, the relative humidity of each measuring point was located near (78±2)%, so the humidity value of the corresponding measuring point can be obtained according to the temperature of different measuring points, thus providing a theoretical basis for the relationship between indoor temperature and humidity.

CONCLUSIONS

This paper analyzed the pattern of temperature and humidity changes in the sunken solar greenhouse. The following conclusions were drawn:

(1) Temperature and humidity relationships during the day in a sunken solar greenhouse were reversed during smothering. There were three phases of temperature change during the day: the rising curve, the fluctuating phase and the falling curve.

(2) The maximum value of indoor temperature at noon was 69.5°C. When the measurement points at the upper surface of the floor were removed, the relative humidity value of other measurement points was less than 60% for a period of 5 h, which can meet the requirements of greenhouse sterilization for high temperature and low humidity environments.

(3) During the 7:00-12:00 time period, when the room temperature was all greater than 28°C and the initial relative humidity values at each measurement point were located between 70% and 85%, the weighted temperature at each measurement point began to rise at a rate of 1.1°C/10min and the weighted humidity at each measurement point fell at a rate of 1.3%/10min. There was a relationship between the temperature and humidity changes in the greenhouse.

ACKOWLEDGEMENT

I am very grateful to Prof. Shuangxi Wang, Prof. Junlin He and Associate Prof. Zhonghua Liu. I am very grateful to the College of Urban and Rural Construction for their help during the experiment and to Shanxi Agricultural University for the PhD start-up costs.

REFERENCES

[1] Cheng Weiwei (2021). *Study on thermal environment and marginal effect of sunken solar greenhouse (下沉式日光温室三维热环境及边际效应的研究).* College of Agricultural Engineering, Shanxi Agricultural University.

[2] Chen P., Wang Y.Z, Liu Q.Z. et al (2020). Phase changes of continuous cropping obstacles in strawberry (Fragaria × ananassa Duch) production[J]. *Applied Soil Ecology*, 155:103626.

[3] Fu G.H., Liu W.K. (2016). Sunlight greenhouse pepper ridging embedded substrate cultivation root zone temperature variation characteristics (日光温室甜椒起垄内嵌式基质栽培根区温度日变化特). *Chinese journal of eco-agriculture,* 24(1):47-55.

[4] Hu Q.Q., LI Y., Lu G.Q. (2015). Effect of high temperature smoking-shed technology on continuous cropping obstacle control of pepper greenhouse (高温闷棚技术对设施辣椒 连作障碍防治效果的研究). *Journal of pepper science,* 13(1): 23-25.

[5] He Z.G., Lou C.R., Dong H. (2018). Effects of straw returning on soil microhabitat and growth and development of tomato under continuous cropping (秸秆还田与高温闷棚对设施连作土壤微生境及番茄生长发育的影响). *Journal of Henan agricultural sciences.* 47(10):87-91.

[6] He Wei, Luo Wenfang, Yu Zhenhua et al (2022). Higher temperature Influence on the control effect of the root-knot nematode and soil microbial community structure of vegetables in the facility (高温闷棚对设施蔬菜根结线虫的防治效果及土壤微生物群落结构的影响). *Xinjiang Agricultural Science*, 59(1):179-189.

[7] Jia W.S., Li M.N., LI Y. (2016). Application of Key Internet Thing Technologies in Facility Agriculture. *Journal of Food Safety and Quality,* 7(11):4401-4407.

[8] Lal R. (2020). Home gardening and urban agriculture for advancing food and nutritional security in response to the COVID-19 pandemic, *Food Secur*. 12 (4): 871–876.

[9] Li J.C. (2015). *Effect of irrigated high temperature smothered shed on soil remediation of continuous cropping in greenhouse (灌水高温闷棚对温室连作土壤修复效果的研究).* Xi'an: College of Horticulture, Northwest A&F University.

[10] Morshed W., Abbas L., Nazha H. (2022). Heating performance of the PVC earth-air tubular heat exchanger applied to a greenhouse in the coastal area of west Syria: An experimental study, *Therm. Sci. Eng. Prog*. 27:101000.

[11] Peng P., Liang L., Li H.L., Zhao G.S. (2019) Current situation, Problems and development suggestions of Facility agriculture in China (我国设施农业现状、问题与发展建议). *Northern Horticulture* (05):161-168.

[12] Shi L.J., Sun J.Q., Cai C. (2021) Methods of swarming greenhouse in Shandong province and matters needing attention (山东地区常用的闷棚方法及注意事项). *Modern Agricultural Science and Technology* (17):88-89.

[13] Sun B., Bai Z., Bao L. et al. (2020). Bacillus subtilis biofertilizer mitigating agricultural ammonia emission and shifting soil nitrogen cycling microbiomes[J]. *Environment International*, 144: 105989.

[14] Ghani S. et al. (2019). Design challenges of agricultural greenhouses in hot and arid environments – A review, *Eng. Agric. Environ*. *Food.* 12 (1):48–70.

[15] Steven W., Van G., Thomas I. (2017). Energy Water and Nutrient Impacts of California-grown Vegetables Compared to Controlled Environmental Agriculture Systems In Atlanta, GA. *Resource, Conservation and Recycling*. 122:319-325.

[16] Wang S.Q., Zhang Z.L., Hou W.N. (2012) Characteristics of soil temperature variation in southern marginal area of sunken solar greenhouse (下沉式日光温室南侧边际区域土壤温度变化特征). *Transactions of the Chinese society of agricultural engineering*. 28 (8): 235-240.

[17] Zhang L.H., Zhang F., Liu S., Xu L. (2010) Three-dimensional unsteady simulation of indoor temperature field of sunken earth wall greenhouse (下沉式土质墙体温室室内温度场的三维非稳态模拟). *Acta Solar Energy Sinica.* (31).